

# AN INSTANT WORKING LEVEL METER WITH AUTOMATIC INDIVIDUAL RADON DAUGHTER READOUT FOR URANIUM MINES<sup>‡</sup>

Peter G. Groer\*, Donald J. Keefe†, William P. McDowell†  
and Richard F. Selman\*

\* Radiological and Environmental Research Division

† Electronics Division

Argonne National Laboratory

Argonne, Illinois

## Abstract

The Instant Working Level Meter (IWLM) evaluates the Working Level and the individual Rn-daughter concentrations in an uranium mine atmosphere within five minutes. The instrument is portable and fully automatic. The WL and the Ra A, Ra B and Ra C concentrations (pCi/liter) are displayed in digital form. Calculation of these quantities is performed by a pre-programmed CMOS calculator chip using the counts observed in the instruments three channels (Ra A, Ra B + C, Ra C'). The Rn-daughters are collected on a membrane filter at a flowrate of 12 liter/min.  $\alpha$ -spectroscopy is performed with a silicon surface barrier detector, the  $\beta + \gamma$  - counts are detected with a plastic scintillator plus PM tube. No assumptions about Rn-daughter equilibrium are made. Only constancy of the Rn-daughter concentrations during the time of sampling (2 minutes) is assumed. The unit is entirely solid state with exception of the photomultiplier. The range of the instrument is 0.01 - 100 WL.

## Introduction

The commonly used methods<sup>1-3</sup> to determine the WL (Working Level) and the short-lived Rn-daughter concentrations in uranium mine atmospheres suffer from several shortcomings. It takes a minimum of 17 minutes to complete the measurements using the fastest of these methods and in the most frequently used procedure<sup>1</sup> the Rn-daughter equilibrium and the influence of the build-up time of the activity on the resulting WL is neglected. The first attempt to solve these problems<sup>4</sup> produced an IWLM (Instant Working Level Meter) which was capable of automatic WL determination but was limited by the low air sampling rate and the high  $\gamma$  -sensitivity of its  $\beta$  -detector. The pseudo-WL due to  $\gamma$  -background has been reduced by about a factor of fifty in the instrument described in this paper. This was achieved by increasing the sampling rate to 12 liter/minute, use of a thinner scintillator (0.003 in.) and shielding of the  $\beta$  -detector.

---

<sup>‡</sup> This research was sponsored by the U.S. Bureau of Mines under Contract No. H0122106.

## Description

### Mechanical Assembly

A schematic drawing of the air sampling system is given in Fig. 1.

After a one minute background counting period and a two minute sampling period, the filter paper tape (Gelman, Acropor, pore size  $0.8\mu$ ) is moved from the air intake by spring tension to position the active area between the  $\alpha$ -detector (ORTEC, silicon surface barrier detector) and the  $\beta$ -scintillator (NE 102). After a delay of three seconds, the two minute counting period starts automatically. After this period, the WL and the Ra A, Ra B and Ra C concentrations in pCi/liter are read out on command. After completion of the measurement the active spot is moved from the counting position and discarded. We found a self-absorption of 0.4% in the filter paper (Gelman, Acropor) using the method of J. Shapiro<sup>5</sup>. A carbon vane pump (GAST) driven by a printed circuit motor delivers a sampling rate of about 12 liter/minute. A tachometer senses the revolutions per minute and is part of a feedback system ensuring constant flow-rate.

### Electronic System

The electronic circuitry consists of three major subsystems: the detection subsystem, a control-computer subsystem and a power subsystem. (See functional block diagram.) The detection subsystem is further broken down into the  $\alpha$ -detection channel and  $\beta$ -detection channel, the pump motor regulator and drive circuit, the high voltage regulator and the solenoid actuator for the paper drive system.

Detection Subsystem. The  $\alpha$ -detection channel consists of a surface barrier detector, a high gain charge sensitive preamplifier, a pulse amplifier, and a single channel analyzer to separate Ra A from Ra C'. The overall  $\alpha$ -detection gain is 5 volts per pC.

The  $\beta$ -detection channel consists of a 10 stage low noise high gain photomultiplier, a NE 102 scintillator, a high gain charge sensitive preamplifier and a discriminator.

Power Subsystem. The power subsystem consists of 13 rechargeable Gel cell batteries and a connector which selects either individual cells for the external charging circuit or combines the batteries into the power pack which consists of an 18 V, 3 Ah battery for operation of the pump, a 6 V, 3 Ah battery for the digital components and  $\pm 12$  V, 1 Ah batteries for the linear components.

Control-Computer Subsystem. The control section of the control-computer subsystem consists of a CMOS driven sequential control circuit which applies the timing pulses for the fully automatic operation.

Also included in the control section are three burst generators, one for each output (Ra A, Ra (B+C) and Ra C'), used to generate double pulses for each single input pulse during the background counting period. These doubled background counts are subtracted from the normal sample count through the use of

up-down counters (accumulators) to compensate for the  $\gamma$  -background. Gamma shielding is achieved through the use of a lead shield (see Fig. 1) and by positioning the batteries around the detector section. The control section also controls the input gating, signal routing and digital resets of the computer section to provide the proper compensated two minute sample count to the accumulators.

The computing subsystem is essentially a pre-programmed buss oriented digital processor. This processor accepts digital data from the accumulators, combines it with various stored constants and from this data calculates Working Level and the individual Rn-daughter concentrations. The processor consists of a MOS calculator circuit, a program memory, a constant memory, a system clock generator, accumulators, calculator driver, display driver, and display as shown in Fig. 2.

The entire circuit except for the memories is assembled from CMOS digital integrated circuits which offer very low power consumption and high immunity to electrical noise.

In order to understand the operation of the circuit, a brief explanation of it's component parts follows:

- 1) The program control section consists of two programmable read only memories (PROM's) which store the program steps, a program counter which advances once for each program step, and a 4 line to 16 line decoder which translates part of the digital word from the memory into individual commands such as add, enter accumulator A, enter constant 5, multiply, etc. The data lines from the PROM's are also used to select the location of a particular constant in the constant memory.
- 2) The constant memory consists of two PROM's which hold the 12 constants required for the calculations; a memory address register which locates and clocks out the constant requested by the program; a set of clock controls; and a set of transmission gates which tie the memories to the data buss. The constant consists of six information words which may include a decimal point. The use of PROM's allows a field change of constants should changes in counting efficiency or flowrate alter the equations.

The information is entered onto the data-buss in a bit-parallel, digit serial fashion. The system clock provides the timing information required to serialize the data. In a particular timing sequence, C0 through C15, the clock pulse C1 steps the program memory register to the next location. If the command at this location calls for entering data from an accumulator, the constant memory or the flowrate correction switch, then clock pulses C2 through C15 enter the data into the calculator. If the new program step called for an operation such as multiply or add, then this operation would be entered into the calculator at time C1. When C1 appears for the second time, the program again advances and new data is entered or a new operation performed.

The clock generator consists of an oscillator driving a binary scaler

whose output is decoded in a 4 line - 16 line decoder to generate clock lines  $C_0 - C_{15}$ . These lines are then routed to the proper locations in the system.

The data buss is terminated in the calculator driver card which shifts the voltage levels from those required by the PROM's to those required by the calculator circuit. After the level shifting, the data buss is decoded in a 4 line to 10 line converter to obtain digit information for the calculator while a separate conversion is performed to obtain the decimal point information. These decoded data are then used to control information inputs to transmission gates which enable the calculator inputs. The calculator is interfaced to a Light Emitting Diode (LED) display for the presentation of data.

### Theory and Calibration of the IWLM

The WL is a linear combination of the short-lived Rn-daughter concentrations as shown in the following equation:

$$WL = 1.052 \times 10^{-4} N_A + 5.908 \times 10^{-5} (N_B + N_C) \quad (1)$$

Therefore, the three unknowns  $N_A$ ,  $N_B$ ,  $N_C$  (atoms/liter) have to be determined to evaluate the WL. This is done by relating these quantities to the counts observed in the three channels of the instrument, as shown below:

$$\begin{aligned} A &= 0.580386 E_A V N_A \\ B + C &= (0.036204 E_B + 0.001584 E_C) V N_A + \\ &+ (0.098134 E_B + 0.006941 E_C) V N_B + \\ &+ 0.131000 E_C V N_C \\ C' &= (0.001584 N_A + 0.006941 N_B + 0.131000 N_C) E_A V \end{aligned} \quad (2)$$

$A$  =  $\alpha$ -counts in RaA - channel  
 $B+C$  =  $\beta+\gamma$  -counts from RaB and RaC  
 $C'$  =  $\alpha$ -counts in RaC' - channel  
 $V$  = flowrate (liter/minute)  
 $E_A$  = detection efficiency for RaA and RaC'  
 $E_B$  = detection efficiency for RaB  
 $E_C$  = detection efficiency for RaC

The numerical coefficients in (2) follow from the laws of radioactive series decay. The half-lives used are:

RaA:  $T_{1/2} = 3.05$  min.  
 RaB:  $T_{1/2} = 26.8$  min.  
 RaC:  $T_{1/2} = 19.7$  min.

For example, the numerical coefficient (0.580386) in the equation for A follows from:

$$(1 - \exp(-\lambda_A t_B)) \exp(-\lambda_A/20) (1 - \exp(-\lambda_A t_D)) / \lambda_A \quad (3)$$

with:

$\lambda_A$  = decay constant of RaA = 0.227621  
 $t_B$  = 2 min. sampling time  
 $t_D$  = 2 min. counting time

The first term in (3) describes the build-up, the second the decay of the RaA activity during the 3 sec. delay and the third the accumulation of counts during the counting period. The analogous coefficients for daughter and granddaughter products are more complex and are not given here.  $E_A$  is determined by comparison with a calibrated hemispherical gas-flow proportional counter.  $E_B$  and  $E_C$  are calculated in the following manner. First  $N_A$ ,  $N_B$  and  $N_C$  are determined from the  $\alpha$ -counts observed using the following equations:

$$\begin{aligned} N_A &= 0.926838 E_A V A(5) \\ N_B &= (-0.879403 A(5) - 11.12606 C'(5) + 2.752840 C'(30)) E_A V \quad (4) \\ N_C &= (0.049957 A(5) + 4.232080 C'(5) - 0.251541 C'(30)) E_A V \\ A(5) &= \text{RaA counts observed during five minutes starting three} \\ &\quad \text{seconds after the end of the two minute sampling time.} \\ C'(5) &= \text{Ra C' counts observed during the same time interval as above.} \\ C'(30) &= \text{Ra C' counts observed during thirty minutes starting three} \\ &\quad \text{seconds after the end of sampling.} \end{aligned}$$

The numerical coefficients in (4) follow again from the laws of radioactive series decay. Since their derivation is straightforward but lengthy, it is not given here. With  $N_A$ ,  $N_B$  and  $N_C$  known  $E_B$  and  $E_C$  can be determined from the following equations:

$$\begin{aligned} BC(5) &= (0.127907 N_A + 0.236138 N_B) V E_B + \\ &\quad + (0.010200 N_A + 0.028418 N_B + 0.311000 N_C) V E_C \\ BC(30) &= (0.981722 N_A + 1.050628 N_B) V E_B + \\ &\quad + (0.385895 N_A + 0.478116 N_B + 1.256959 N_C) V E_C \quad (5) \\ BC(5) &= \text{total } \beta \text{-counts observed during five minutes starting three} \\ &\quad \text{seconds after the end of sampling.} \\ BC(30) &= \text{total } \beta \text{-counts observed during thirty minutes starting} \\ &\quad \text{three seconds after the end of sampling.} \end{aligned}$$

With  $E_A$ ,  $E_B$  and  $E_C$  so determined, equations (2) can be inverted. Properly scaled the inverted equations give the Rn-daughter concentrations in pCi/liter and the WL as a linear combination of A, B + C and C'. These inverted equations are programmed in the calculator subsystem of the IWLM. It is clear from this description of the calibration that the IWLM determines the Rn-daughter concentrations and the WL without any assumptions about Rn-daughter equilibrium. Since all weighing coefficients are strictly proportional to  $1/V$ , a flow-rate variation can be easily corrected for. This correction is accomplished by setting the ratio (calibration flowrate/observed flowrate) on a thumb wheel switch indicated in Fig. 2. Recalibration of the IWLM, if used at different elevations or with different flowrates, is therefore unnecessary.

### Tests

We tested a prototype IWLM in the experimental Dakota Mine in New Mexico. The results are shown below:

Test	IWLM				$\alpha$ -Spectroscopic Method (See Eq. (3))				Kusnetz Method
	WL	RaA (pCi/litre)	RaB (pCi/litre)	RaC (pCi/litre)	WL	RaA (pCi/litre)	RaB (pCi/litre)	RaC (pCi/litre)	
1	0.88	173	85	68	0.83	171	80	66	0.85
2	1.44	231	129	140	1.51	233	150	137	1.58
3	1.11	219	104	92	1.12	217	109	91	1.12
4	1.47	292	149	105	1.44	296	146	107	1.43
5	0.71	110	69	63	0.76	142	73	64	0.71
6	0.32	74	33	21	0.31	76	30	20	0.31
7	0.52	89	62	28	0.40	90	38	29	0.44

WL, RaA and RaC concentrations determined by the IWLM and the spectroscopic method are in good agreement. The same is true for the RaB concentrations in most cases. The reasons for deviations like in Test 2 and 7 are not clear. More tests are needed to clarify these discrepancies.

#### References

1. H. L. Kusnetz, Am. Ind. Hyg. Assoc. Quart. 17, 85 (1956).
2. E. C. Tsivoglou, H. E. Ayer and D. A. Holaday, Nucleonics 11, 40 (1953).
3. J. Thomas, Health Physics 19, 691 (1970).
4. P. G. Groer, R. D. Evans and D. A. Gordon, Health Phys. 24, 387 (1973).
5. J. Shapiro, Univ. of Rochester, Report UR-298 (1954).

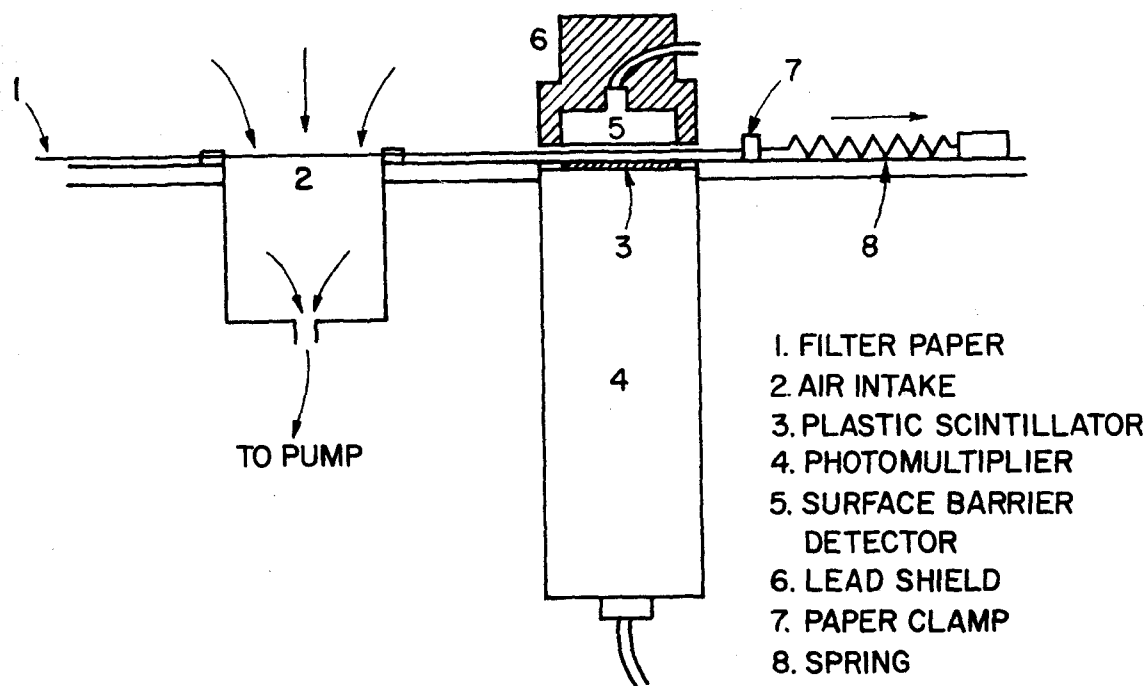


Fig. 1 Detection, air sampling and paper transport mechanisms of the IWLM.

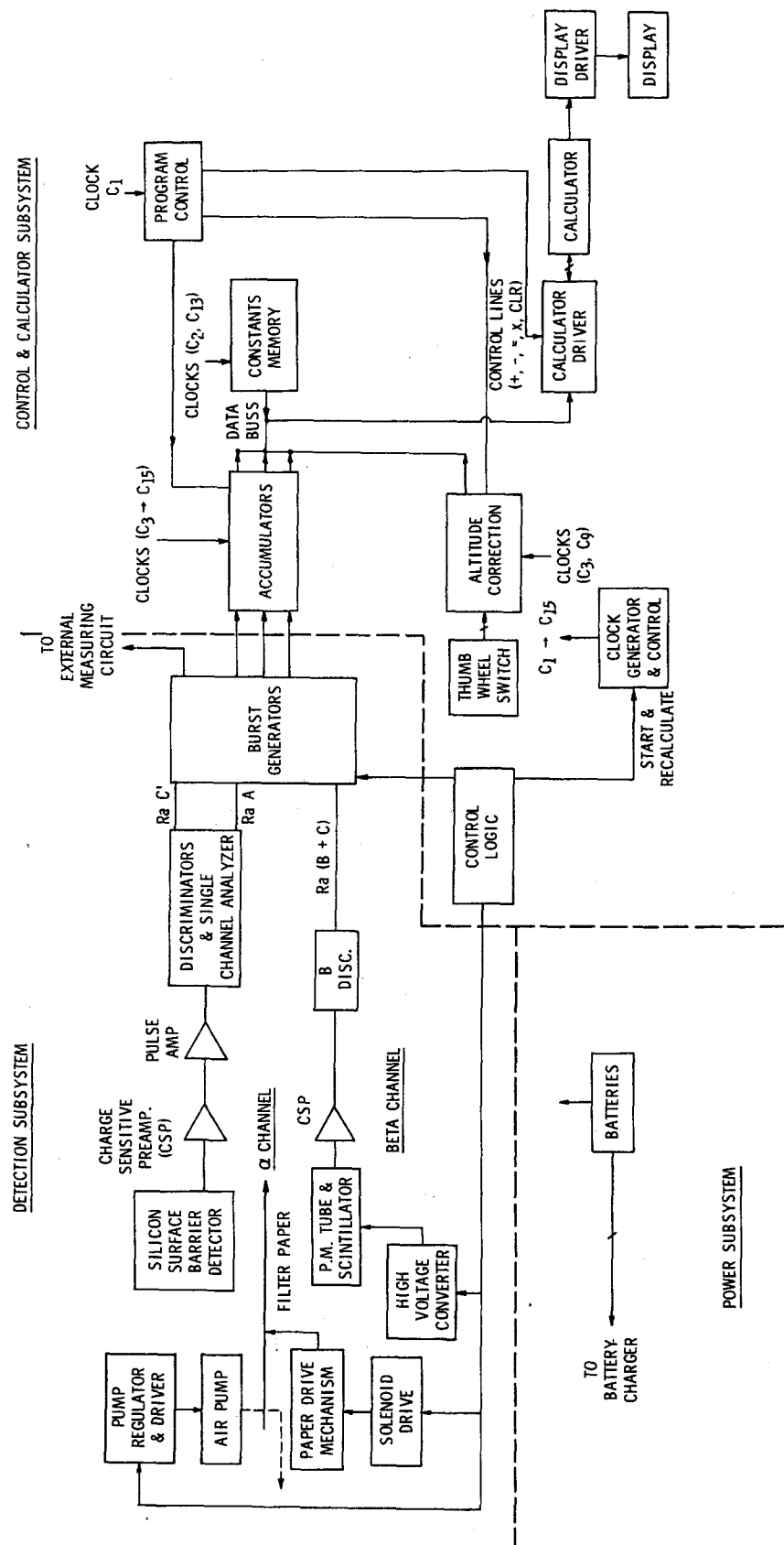


Fig. 2 Functional block diagram of the IWLM.